Archives of Medical Reports

2(4) (2025) 22-33

OPEN ACCESS

RESEARCH ARTICLE

Betanin Conjugated Silica Nanoparticles as a Novel Therapeutic Strategy Against Multidrug Resistant Opportunistic Pathogens

Praveena Vijaya Devan [1,*], Mehwish Shoaib [2]

[1] University of Cyberjaya, Persiaran Bestari, Cyber 11, 63000 Cyberjaya, Selangor, Malaysia.

[2] Moti Lal Nehru Medical College, George Town, Prayagraj-211002, Uttar Pradesh.

***Corresponding Author:** Praveena Vijaya Devan
University of Cyberjaya, Persiaran Bestari, Cyber 11, 63000 Cyberjaya, Selangor, Malaysia.
Email: vjpraveena83@gmail.com

Articleinfo
Received: 28 April 2025
Accepted: 25 June 2025

Keywords: Betanin; Silica Nanoparticle; Multi Drug Resistant; Antimicrobial

How to cite this article: Praveena Vijaya Devan. (2025). Betanin Conjugated Silica Nanoparticles as a Novel Therapeutic Strategy Against Multidrug Resistant Opportunistic Pathogens, 2(4), 22-33 Retrieved from https://archmedrep.com/index.php/amr/article/view/58

Abstract

Betanin (BT), a natural pigment with antioxidant, antimicrobial, and anticancer properties, was explored in combination with silica nanoparticles (SiNPs) to develop a biocompatible formulation with enhanced bioactivity. This study reports the synthesis and characterization of BT-SiNPs using UV-Vis spectroscopy, SEM, FTIR, and XRD techniques. The antioxidant activity of BT-SiNPs was evaluated through superoxide and hydroxyl radical scavenging assays, demonstrating significant dose-dependent activity. The antimicrobial potential of BT-SiNPs was assessed against major respiratory pathogens, including *Salmonella typhi, Listeria monocytogenes,* and *Escherichia coli*, using minimum inhibitory concentration (MIC) and zone of inhibition assays. The results showed significant antimicrobial efficacy, with an MIC of 50 µg/mL. Molecular docking studies revealed strong interactions between BT and pathogen receptors, suggesting inhibition of quorum sensing and antibiotic resistance mechanisms. In conclusion, BT-SiNPs exhibit antioxidant and antimicrobial activity making them potential candidates for therapeutic applications against oxidative stress, respiratory infections, and lung cancer.

1. Introduction

The rapid emergence and global spread of multidrug resistant pathogens is one of the most serious challenges in modern medicine. Infections caused by multidrug resistant bacteria are associated with prolonged illness, higher rates of morbidity and mortality, and increased economic burden due to extended hospital stays and costly treatment regimens (Alara and Alara, 2024). According to the World Health Organization, antimicrobial resistance has reached alarming levels in both developed and developing nations, threatening the efficacy of available antibiotics. The situation is particularly concerning in the case of opportunistic bacterial pathogens such as *Salmonella typhi*, *Listeria monocytogenes,* and Escherichia coli, which are major contributors to foodborne and systemic infections (Kim et al., 2014; Robi et al., 2024). *S. typhi* is the causative agent of typhoid fever, a systemic infection that continues to pose a significant health burden in many low- and middle-income countries. The organism has developed resistance to multiple first-line antibiotics including chloramphenicol, ampicillin, and trimethoprim-sulfamethoxazole, and more recently to fluoroquinolones and third-generation cephalosporins (Klemm et al., 2018). Similarly, *L. monocytogenes*, a foodborne pathogen responsible for listeriosis, exhibits natural resistance to several antibiotics and has shown growing resistance to commonly used antimicrobials such as tetracycline and erythromycin (Conter et al., 2009). Listeriosis is of particular concern in immunocompromised individuals, neonates, and pregnant women, where it can cause severe systemic infections, meningitis, and even fetal loss (Schlech, 2019). *E. coli*, one of the most widely studied bacterial species, includes both commensal and pathogenic strains. The prevalence of extended-spectrum beta-lactamase (ESBL)-producing E. coli strains highlights the magnitude of resistance (Padmini et al., 2017), making standard antibiotics such as penicillins and cephalosporins ineffective.

The treatment challenges associated with these pathogens highlight the need for novel therapeutic agents that can overcome multidrug resistance. Natural bioactive compounds derived from plants have attracted increasing attention as potential alternatives or adjuvants to conventional antibiotics. Betanin (BT) is the major pigment found in red beetroot (*Beta vulgaris*), and it is well recognized for its antioxidant, anti-inflammatory, and antimicrobial properties (Starzak et al., 2021). Studies have demonstrated that BT can interfere with bacterial growth by inducing oxidative stress, disrupting cell membrane integrity, and inhibiting essential enzymes (Mbae and Umesha, 2020). In addition, BT possesses the ability to modulate host immune responses, thereby enhancing the overall defense mechanism against infections. However, the clinical application of BT is limited due to its poor stability, susceptibility to degradation under environmental conditions such as light and heat, and low bioavailability. These limitations hinder its therapeutic efficacy when used in free form. To address these challenges, nanotechnology-based approaches have been explored to improve the delivery, stability, and bioactivity of natural compounds like BT. Among various nanocarriers, silica nanoparticles (SiNPs) have emerged as highly versatile and biocompatible delivery systems. They are non-toxic at appropriate concentrations, biodegradable, and have been widely studied for biomedical applications including drug delivery, imaging, and biosensing (Hoang Thi et al., 2019; Hosseinpour et al., 2020). The conjugation of BT with SiNPs offers a promising strategy to overcome the limitations of free betanin while enhancing its antimicrobial potential. By encapsulating or attaching betanin onto the surface of SiNPs, the compound can be protected from premature degradation, thereby prolonging its stability and activity. This approach also improves solubility and bioavailability, ensuring that therapeutic concentrations of BT can be achieved at the site of infection. The present study explores the synthesis and evaluation of BT-SiNPs as a novel therapeutic strategy against multidrug resistant S. typhi, L. monocytogenes, and E. coli. By integrating the natural antimicrobial activity of BT with the advanced delivery capabilities of SiNPs, this research aims to establish a foundation for alternative therapeutic approaches to combat multidrug resistant opportunistic pathogens. The findings from this study could contribute to the growing field of nano-bioactive conjugates, offering a safe, effective, and sustainable solution to the pressing problem of antimicrobial resistance.

2. Materials and Methods

2.1. Synthesis of BT-SiNPs

The synthesis of BT-SiNPs was performed through a green synthesis method. Initially, 0.1 M tetraethyl orthosilicate (TEOS) was hydrolyzed in ethanol under constant stirring, followed by the addition of 0.1 M ammonium hydroxide as a catalyst to promote SiNPs formation. Separately, an aqueous BT solution was prepared, and it was slowly introduced into the SiNPs suspension under continuous stirring to allow functionalization. The mixture was incubated at room temperature for 24 hours to ensure uniform coating. The resulting BT-SiNPs were centrifuged, washed with deionized water to remove unbound BT, dried at 60 °C, and stored for further analysis (Henrique Vieira de Almeida Junior et al., 2024).

2.2. Characterization of Synthesized BT-SiNPs

The optical properties of the BT-SiNPs were analyzed using UV–Vis spectrophotometry (UV-1800, Shimadzu) to confirm nanoparticle synthesis. Functional groups present in the BT-SiNPs were identified through Fourier-transform infrared (FT-IR) spectroscopy (Perkin Elmer, USA), within the frequency range of 400–4000 cm^{-1}. The average size, morphology, and crystal structure of the BT-SiNPs were examined using X-ray Diffraction (XRD) and scanning electron microscopy (SEM) (JEOL JSM-. 7800F, Japan) (Babu et al., 2018).

2.3. Superoxide anion and Hydroxyl Radical Scavenging Assay for BT- SiNPs

For the superoxide radical scavenging assay, 1 mL of 0.1 mM nitroblue tetrazolium (NBT) solution was mixed with 1 mL of the test sample (BT-SiNPs) at varying concentrations. Then, 1 mL of 0.1 mM phenazine methosulfate (PMS) solution and 1 mL of 0.1 mM NADH were added. The mixture was incubated at 25 °C for 10 minutes in the dark. The reaction was stopped by adding 1 mL of 2 M HCl, and absorbance was measured at 560 nm using a spectrophotometer (Pradhan et al., 2021).

The hydroxyl radical scavenging assay for BT-SiNPs was performed utilizing the Fenton reaction to generate hydroxyl radicals (Hassan et al., 2024). The procedure included mixing 1 mL of 0.1 mM iron (II) sulfate solution with 1 mL of 1 mM hydrogen peroxide (H_2O_2) and 1 mL of BT-SiNPs at various concentrations. The reaction was triggered by the addition of 1 mL of deionized water, followed by incubation at 37 °C for 30 minutes. Subsequently, 1 mL of 0.75 mM salicylic acid was added, and the mixture was incubated at room temperature for 1 hour to allow complex formation. The scavenging activity of the BT-SiNPs against hydroxyl radicals was assessed by measuring the absorbance of the solution at 510 nm using a microplate reader.

2.4. Antimicrobial activity of BT-SiNPs

To evaluate the antimicrobial activity of BT-SiNPs, the Minimum Inhibitory Concentration (MIC) assay and the zone of inhibition assay were performed. For the MIC assay, respiratory tract bacterial strains, such as *S. typhi*, *L. monocytogenes*, and *E. coli* were cultured in Mueller-Hinton broth (MHB) and adjusted to 1.5×10^8 CFU/mL. Serial dilutions of BT-SiNPs were prepared in 96-well microplates, with concentrations ranging from 5 µg/mL to 100 µg/mL. Each well was inoculated with 100 µL of bacterial suspension, and the plates were incubated at 37°C for 24 hours. After incubation, the MIC was determined by observing the lowest concentration of BT-SiNPs that completely inhibited visible bacterial growth, indicated by the absence of turbidity in the wells. Control wells without BT-SiNPs and those containing Ciprofloxacin as a positive control were also included for comparison (Parvekar et al., 2020).

For the zone of inhibition assay, the agar well diffusion method was used. Bacterial cultures were uniformly spread onto Mueller-Hinton agar (MHA) plates using sterile cotton swabs. Wells (6 mm in diameter) were produced in the agar, and 100 µL of BT-SiNPs at varying concentrations (e.g., 50 µg/mL, 100 µg/mL) were added to each well. The plates were incubated at 37° C for 24 hours, and the zones of inhibition were measured in millimeters using a caliper. Ciprofloxacin was used as a positive control, and sterile distilled water was used as a negative control. The antimicrobial effectiveness of the BT-SiNPs was assessed by comparing the size of the inhibition zones across different bacterial strains (Ahmad et al., 2024).

2.5. Molecular Docking

Molecular docking simulations were carried out using AutoDock to determine the binding affinity of betanin with proteins from respiratory pathogens. The 3D structures of target proteins from *S. typhi, L. monocytogenes,* and *E. coli* were retrieved from the Protein Data Bank (PDB) and assessed using PyMOL for structural evaluation and preparation. Protein structures were prepared by eliminating water molecules and non-essential ligands, followed by the addition of polar hydrogens. The BT ligand was obtained from the PubChem database in SDF format and converted to mol2 format using OpenBabel for compatibility. AutoDock Tools were used to prepare the ligand and receptor by adding Gasteiger charges and setting up the grid box parameters. Docking was performed with AutoDock Vina, and binding affinities were calculated in kcal/mol. Multiple binding poses were generated, with the best pose selected based on the lowest binding energy. The docked complexes were analyzed using Discovery Studio Visualizer to identify key interactions, such as hydrogen bonding and hydrophobic contacts, between betanin and the amino acid residues of the target proteins, supporting its potential as an inhibitor of respiratory pathogens (Aytar et al., 2024).

2.6. Statistical analysis

The results are expressed as the mean ± standard deviation from three independent experiments. Graphs were generated using GraphPad Prism software. Statistical analysis was conducted using one-way ANOVA, followed by post-hoc tests to assess significant differences between the control and treatment groups.

3. Results

3.1. Characterization of synthesized BT-SiNPs

The UV-Vis absorption spectrum of the synthesized BT-SiNPs exhibited a distinct absorption peak in the range of 200–250 nm, which validates the effective synthesis of the NPs. The sharp peak indicates the presence of uniform NPs, which is consistent with the predicted optical properties of SiNPs. The lack of significant absorption further than 250 nm implies reduced aggregation, confirming that the NPs retain their optical characteristics (Figure 1). The SEM result was observed with uniformed spherical shape NPs (Figure 2). The XRD analysis of BT-SiNPs reveals a predominantly amorphous nature (71.5%) with a minor crystalline phase (28.5%). The broad hump in the pattern confirms the amorphous silica matrix, while sharp peaks at 31.619°, 42.232°, and 45.457° indicate some retained crystallinity, possibly from residual betanin or silica interactions (Figure 3). The FTIR analysis of BT-SiNPs identified key functional groups linked to the bioactive coating and confirmed the successful synthesis of NPs. Prominent peaks were observed at 3279 cm^{-1}, corresponding to O-H stretching vibrations, and at 2932 cm^{-1}, indicative of C-H stretching. The bands at 1563 cm^{-1} and 1404.9 cm^{-1} were linked to aromatic C=C stretching and symmetric/asymmetric vibrations of carboxylate groups, respectively. Additional bands at 1337 cm^{-1} and 1020.5 cm^{-1} confirm C-O stretching, while peaks below 927 cm^{-1} represent Si-NP interactions (Figure 4). These functional groups confirm the presence of BT on the NP's surface, indicating successful coating.

3.2. Antioxidant potential of BT-SiNPs

The hydroxyl radical scavenging activity of BT-SiNPs was evaluated and compared with ascorbic acid

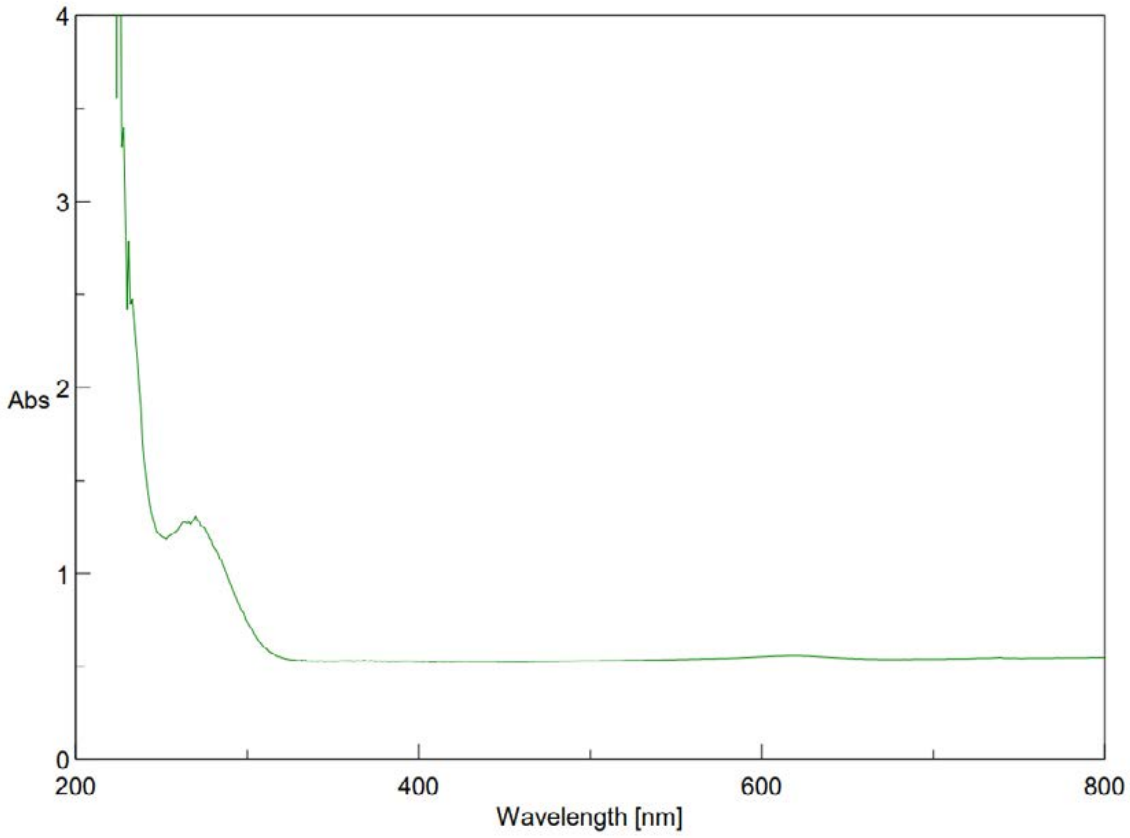

Figure 1: UV-Vis absorption spectrum of the synthesized BT-SiNPs complexes shows a distinct peak in the 200–250 nm range, confirming nanoparticle synthesis.

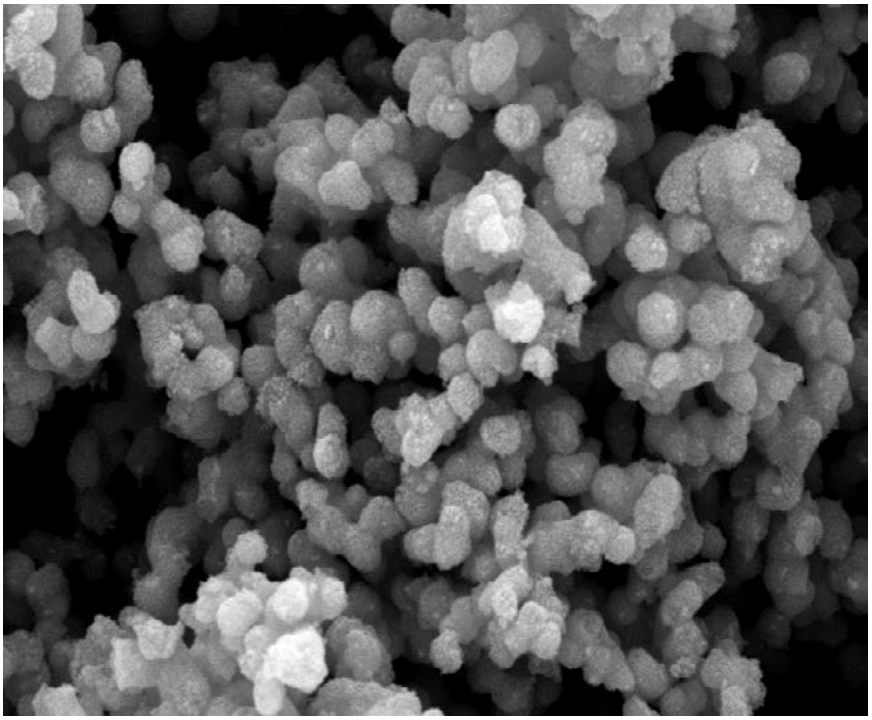

Figure 2: SEM analysis of nanoparticle showing spherical shape

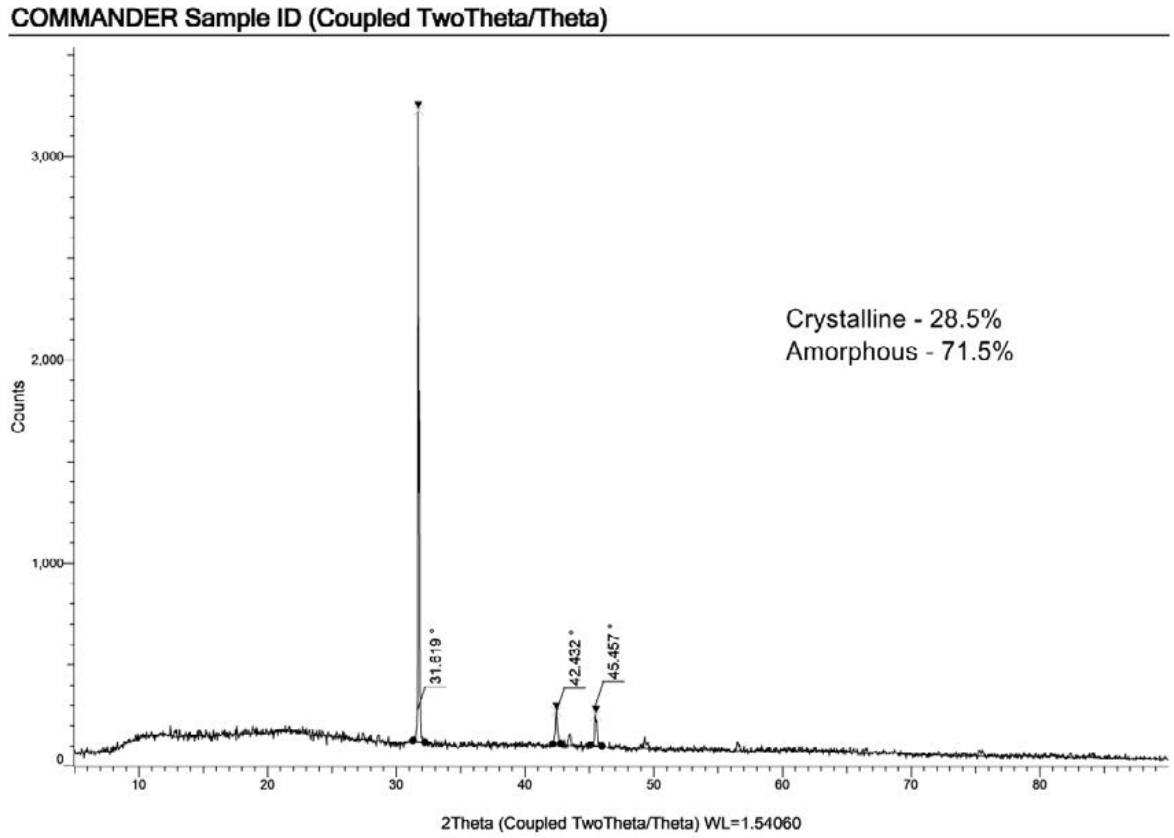

Figure 3: XRD analysis of BT-SiNPs complexes indicating the presence of both crystalline and amorphous phases.

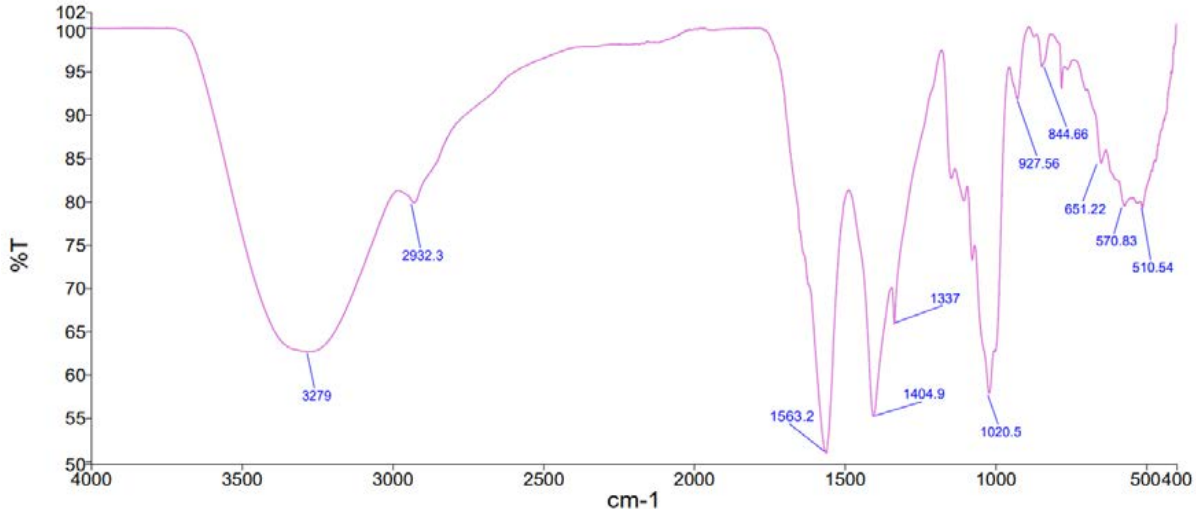

Figure 4: FT-IR spectrum demonstrates the characteristic vibrational modes of the functional groups present in the BT-SiNPs complexes

as a standard antioxidant. The results demonstrated a concentration-dependent increase in scavenging activity for both BT-SiNPs and ascorbic acid. At the lowest concentration of 5 µg/mL, BT-SiNPs exhibited 5 % activity, while ascorbic acid showed higher activity at 8.5 %. This trend was consistent across all tested concentrations, with BT-SiNPs showing a scavenging activity of 61.5 % at 100 µg/mL, which was comparable to the 69.5 % scavenging activity of ascorbic acid at the same concentration (Figure 5A). The results demonstrate that BT-SiNPs display significant hydroxyl radical scavenging activity, especially at higher concentrations, highlighting their potential as powerful antioxidant agents. While ascorbic acid consistently exhibited higher activity, the comparable performance of BT-SiNPs at elevated concentrations validates their potential for mitigating oxidative stress.

The superoxide anion radical scavenging activity of BT-SiNPs was assessed and compared to ascorbic acid as a standard antioxidant. The results demonstrated a concentration-dependent increase in scavenging activity for both BT-SiNPs and ascorbic acid. At 5 µg/mL, BT-SiNPs exhibited 6.5% scavenging activity, while ascorbic acid showed 14%. At higher concentrations of 25, 50, and 100 µg/mL, BT-SiNPs achieved 28.5%, 53.5%, and 77.5% activity, respectively, compared to 31.5%, 62%, and 86.5% for ascorbic acid (Figure 5B). Although slightly lower than ascorbic acid, the BT-SiNPs demonstrated significant antioxidant potential, indicating their ability to scavenge superoxide radicals effectively.

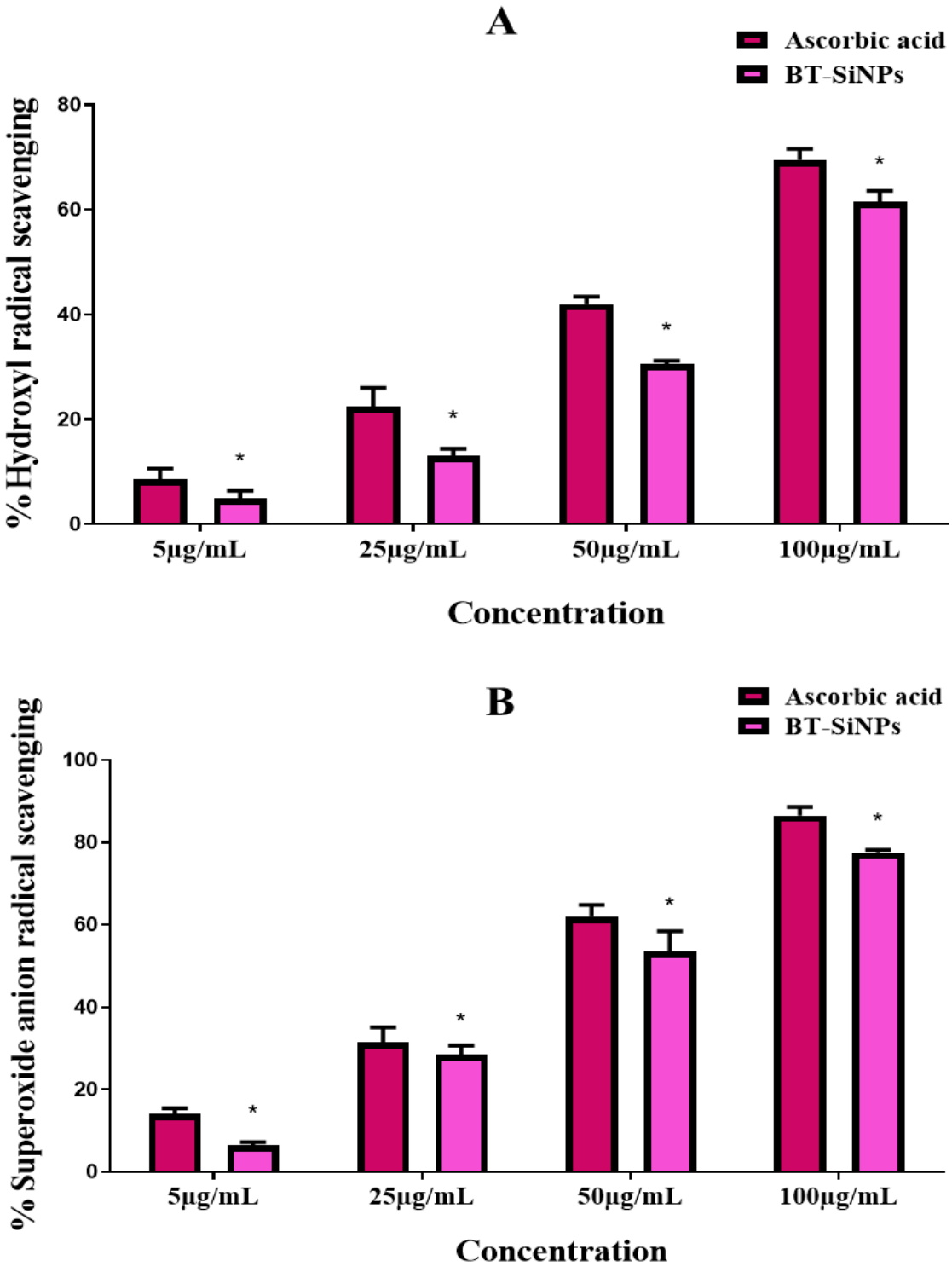

Figure 5. Antioxidant activity of BT-SiNPs was evaluated using (A) superoxide anion radical and (B) Hydroxyl radical scavenging activity of BT-SiNPs was tested at doses of 5, 25, 50, and 100 µg/mL. Ascorbic acid was used as a positive control.

3.3. Antimicrobial potential of BT-SiNPs

The minimum inhibitory concentration (MIC) of BT-SiNPs against *S. typhi, L. monocytogenes*, and *E. coli* was evaluated at concentrations ranging from 5 µg/mL to 100 µg/mL. The antimicrobial efficacy of BT-SiNPs increased in a dose-dependent manner across all tested pathogens. At the highest concentration (100 µg/mL), BT-SiNPs demonstrated significant inhibition, with efficacy comparable to the standard antibiotic Ciprofloxacin (100 µg/mL). In particular, the inhibition percentages for *S. typhi, L. monocytogenes*, and *E. coli* were 79%, 81%, and 65.5%, respectively. At the lowest concentration (5 µg/mL), BT-SiNPs exhibited moderate activity, with inhibition rates of 18%, 21%, and 19.5%, respectively, against *S. typhi, L. monocytogenes,* and *E. coli* (Figure 6A).

The zone of inhibition assay demonstrated that BT-SiNPs exhibited a dose-dependent antibacterial effect. At a concentration of 50 µg/mL, the inhibition zones recorded were 4 mm for *S. typhi*, 7 mm for *L. monocytogenes*, and 3 mm for *E. coli*. When the concentration was increased to 100 µg/mL, the inhibition zones increased significantly, measuring 9 mm for *S. typhi,* 13 mm for *L. monocytogenes,* and 6 mm for *E. coli* (Figure 6B). In comparison with ciprofloxacin (100 µg/mL), which served as the positive control, BT-SiNPs showed comparable activity, particularly against *L. monocytogenes*. These results demonstrate the potential of BT-SiNPs as a promising antimicrobial agent, capable of inhibiting bacterial growth effectively at higher concentrations.

A

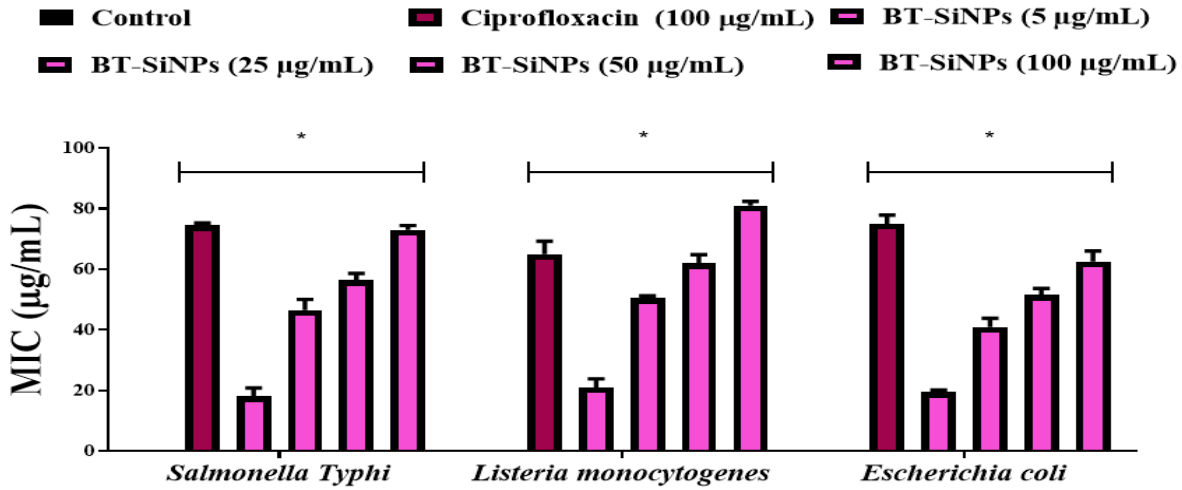

B

Zone of Inhibition (mm)				
Bacterial Strain	**Control**	**Ciprofloxacin 100 µg/mL**	**BT-SiNPs 50 µg/mL**	**BT-SiNPs 100 µg/mL**
Salmonella typhi	-	8	4	9
Listeria monocytogenes	-	7	7	13
Escherichia coli	-	10	3	6

Figure 6: A) Minimum inhibitory concentrations of BT-SiNPs against *S. typhi, L. monocytogenes*, and *E. coli* were determined, with ciprofloxacin used as the positive control. Data are presented as the mean ± standard error based on results from three independent experiments. B) Antimicrobial activity of BT-SiNPs against various respiratory tract pathogens including *S. typhi, L. monocytogenes*, and *E. coli.* Inhibition zones are measured in millimeters (mm).

3.4. Molecular Docking and Binding Affinity Analysis of BT with Multidrug Resistant Pathogen Receptors

The molecular docking study investigated the binding affinity of BT with receptors from multidrug resistant pathogens. Table 1 represents the binding affinity values and amino acid interactions between BT and the receptors of key multidrug resistant pathogens, with a focus on the interaction dynamics at the molecular level. Binding affinity values, expressed in kcal/mol, indicate the strength of the interaction between BT and each receptor. Lower values suggest a stronger binding interaction, with the receptor-ligand complex being more stable. Table 1 demonstrates that BT interacts with the respiratory tract pathogens' receptors, which may have implications for the development of therapeutic interventions targeting these pathogens. Specifically, the receptor proteins in *S. typhi* (outer membrane protein F; PDB ID: 4KR4), *L. monocytogenes* (Listeriolysine-O; PDB ID: 4CDB), *E. coli* (DNA Polymerase II; PDB ID: 1Q8I) show varying degrees of binding affinity, each involving distinct amino acid residues.

The binding affinity of BT with S. typhi (outer membrane protein F; PDB ID: 4KR4) is -4.2 kcal/mol, which indicates a relatively moderate interaction with this receptor. The amino acid residues involved in the interaction are ARG, ASP, TYR, LYS, and ARG (Figure 7). In contrast, the interaction between BT and *L. monocytogenes* (Listeriolysine-O; PDB ID: 4CDB) exhibits a stronger binding affinity of -4.9 kcal/mol, indicating a more stable complex. The amino acid interactions, including SER, VAL, GLU, ASP, TYR, and LYS, are distributed across different regions of the receptor, indicating that BT could potentially inhibit Listeriolysine-O. Finally, the binding interaction of BT with *E. coli* (DNA Polymerase II; PDB ID: 1Q8I) reveals a weaker binding affinity of -3.1 kcal/mol. The key amino acids involved in the interaction include ILE, VAL and GLY, suggesting a more limited interaction compared to the other two receptors. This relatively weaker interaction may imply that BT could be less effective in CIFA modulating metabolic pathways critical for bacterial survival and growth. This strong interaction could lead to the development of BT derivatives as effective antimicrobial agents against *E. coli.*

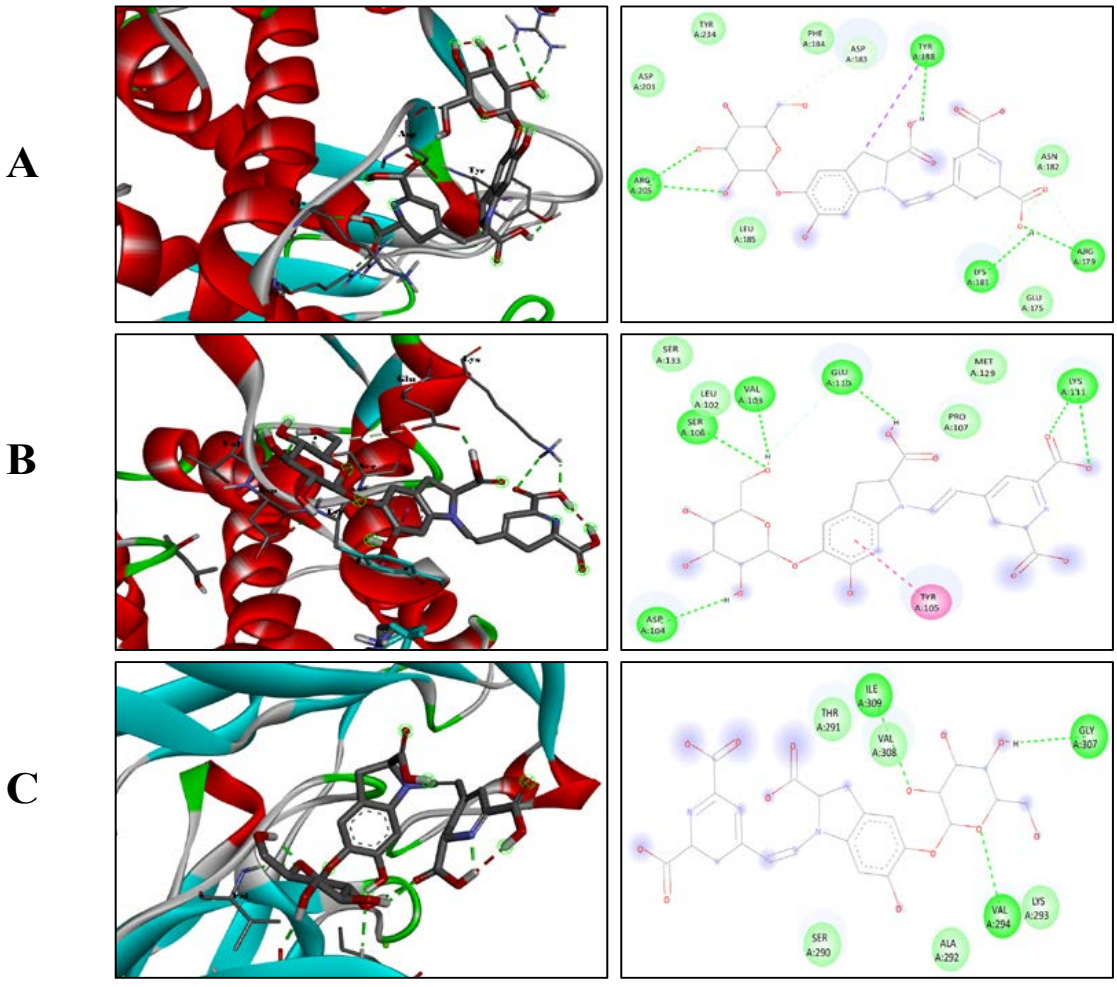

Figure 7: Interaction of BT with the receptors of multidrug resistant pathogens illustrated in both 3D and 2D visualizations. (A) *S. typhi*: Outer membrane protein F, (B) *L. monocytogenes:* Listeriolysine-O, and (C) *E. coli*: DNA Polymerase II

Table 1: Binding affinity value and amino acid interaction between the BT and multidrug resistant pathogens receptors. The amino acid interactions are TYR (Tyrosine), SER (Serine), LYS (Lysine), GLU (Glutamic acid), VAL (Valine), ARG (Arginine), ILE (Isoleucine), GLY (Glycine), and ASP (Aspartic acid)

	Receptor (PDB ID)	Ligand	Binding affinity (kcal/mol)	Amino acid interaction
1	*Pseudomonas aeruginosa*: LasB (3DBK)	Betanin	-4.2	ARG, ASP, TYR, LYS, ARG
2	*Klebsiella pneumoniae:* β-lactamase (1N9B)	Betanin	-4.9	SER, VAL, GLU, ASP, TYR, LYS
3	*Staphylococcus aureus:* ClFA (1N67)	Betanin	-3.1	ILE, VAL and GLY

4. Discussion

The present study demonstrated that BT-SiNPs possess strong antioxidant and antimicrobial activities against multidrug resistant opportunistic pathogens such as *S. typhi, L. monocytogenes*, and *E. coli.* The results suggest that combining a natural bioactive pigment like BT with a nanocarrier such as SiNPs provides a promising therapeutic strategy for combating antimicrobial resistance. The findings are significant, as these pathogens continue to cause severe infections globally and are increasingly resistant to first-line antibiotics. The physicochemical characterization confirmed the successful synthesis of BT-SiNPs. UV–Vis spectroscopy revealed a sharp absorption peak between 200–250 nm, indicating well-dispersed NPs with minimal aggregation. SEM imaging confirmed a spherical and uniform morphology, which is important because particle shape and size strongly influence biological interactions and antimicrobial activity. The XRD pattern demonstrated a predominantly amorphous nature of the NPs, with some minor crystalline phases. Amorphous SiNPs are known to have higher surface reactivity, which enhances functionalization and bioactive loading. FTIR analysis identified functional groups of betanin such as O–H, C–H, carboxylates, and aromatic C=C bonds, proving that BT was successfully coated onto the SiNPs surface. These results support earlier studies showing that SiNPs are excellent carriers for natural compounds due to their high surface area, stability, and ease of surface modification (AbouAitah et al., 2018).

The antioxidant potential of BT-SiNPs was demonstrated through hydroxyl radical and superoxide anion scavenging assays. Both assays showed concentration-dependent activity. While ascorbic acid consistently performed better, BT-SiNPs achieved comparable scavenging capacity at higher concentrations. This finding is particularly important because oxidative stress plays a major role in infection progression. MDR bacteria often produce reactive oxygen species (ROS) as part of their pathogenesis, and excessive ROS can damage host cells, suppress immune function, and worsen clinical outcomes (Song et al., 2025). BT, being a betalain pigment, contains phenolic hydroxyl groups capable of donating hydrogen atoms to neutralize free radicals (Gliszczyńska-Świgło et al., 2006). However, free BT has low stability and bioavailability in biomedical application. The conjugation with SiNPs appears to have protected BT from degradation and allowed sustained antioxidant activity. Similar results have been reported with curcumin-loaded SiNPs, which showed enhanced stability and stronger antioxidant effects compared to free curcumin (Elbialy et al., 2020; Kong et al., 2019). This suggests that SiNPs-based delivery systems can extend the pharmacological potential of natural antioxidants.

The antimicrobial results demonstrated that BT-SiNPs effectively inhibited the growth of *S. typhi, L. monocytogenes*, and *E. coli* in a dose-dependent manner. At 100 µg/mL, BT-SiNPs displayed inhibition comparable to ciprofloxacin, especially against *L. monocytogenes*. This strong activity against *L. monocytogenes* is significant, as listeriosis is notoriously difficult to treat due to its intracellular lifestyle and resistance to several antibiotics (Baquero et al., 2020). The zone of inhibition assay further confirmed these findings, showing larger inhibition zones with higher concentrations of BT-SiNPs. Interestingly, E. coli was less sensitive than the other pathogens, which may reflect differences in outer membrane composition or efflux mechanisms (Masi et al., 2017). The antimicrobial effect of BT-SiNPs can be explained by multiple mechanisms. BT itself possesses antimicrobial activity, attributed to its ability to disrupt bacterial cell membranes, inhibit enzymes, and induce oxidative stress (Mbae and Umesha, 2020). Meanwhile, SiNPs can directly interact with bacterial membranes, leading to structural damage, leakage of cellular contents, and increased permeability (Mathelié-Guinlet et al., 2017). When BT is conjugated to SiNPs, these effects are amplified. The SiNPs act as carriers that facilitate the transport of BT across bacterial barriers and ensure sustained release at the site of action. Furthermore, SiNPs can penetrate bacterial biofilms, which are highly resistant to conventional antibiotics. Previous studies have shown that plant-derived compounds such as quercetin and rutin exhibit enhanced antimicrobial activity when loaded onto SiNPs (Abbasi et al., 2023; Yi et al., 2024), supporting the findings of the current study.

The molecular docking analysis provided additional insights into the potential molecular targets of BT. Docking studies revealed that BT interacts with outer membrane protein F in *S. typhi*, listeriolysin-O in *L. monocytogenes,* and DNA polymerase II in *E. coli.* The binding affinities varied, with the strongest interaction observed for L. monocytogenes. Listeriolysin-O is a pore-forming toxin essential for the escape of L. monocytogenes from the phagosome into the cytoplasm (Schnupf and Portnoy, 2007). By binding to this protein, BT may inhibit its activity, thereby reducing virulence. The moderate binding to *S. typhi* outer membrane protein F suggests interference with nutrient uptake or membrane integrity (Roy Chowdhury et al., 2022). The weaker binding to *E. coli* DNA polymerase II correlates with the lower antimicrobial activity observed experimentally, suggesting that BT is less effective at targeting essential enzymes in *E. coli.* These findings are consistent with recent computational studies that demonstrated selective binding of plant-derived bioactives to bacterial virulence proteins, which can explain pathogen-specific effects.

5. Conclusion

This study demonstrates that BT-SiNPs combine the antioxidant and antimicrobial potential of a natural pigment with the stability and delivery benefits of nanotechnology. The strong activity against *L. monocytogenes* and *S. typhi* and moderate effects against *E. coli* highlight their potential as alternative therapeutics for MDR infections. The dual action of BT-SiNPs suggests they could play a role not only in direct bacterial inhibition but also in reducing oxidative stress-related damage during infection. With further optimization and validation, BT-SiNPs may represent a safe and effective nanoplatform for managing multidrug resistant bacterial infections.

Declarations

Ethics approval statement

Not applicable

Consent to participate

Not applicable

Consent to publish

Not applicable

Data Availability Statement

The data are available from the corresponding author upon reasonable request

Competing Interests

The authors declare that they have no conflict of interest

Funding

Not Applicable

Author contribution

Conceptualization, Data curation, Investigation, & Writing: P.V.D. Formal analysis and Editing: M.S. All authors have read and agreed to the published version of the manuscript`

Acknowledgements

Not Applicable

References

1. Lahiri A, Maji A, Potdar PD, Singh N, Parikh P, Bisht B, Mukherjee A, Paul MK. Lung cancer immunotherapy: progress, pitfalls, and promises. Molecular cancer. 2023 Feb 21;22(1):40.
2. Feng J, Zhang P, Wang D, Li Y, Tan J. New strategies for lung cancer diagnosis and treatment: applications and advances in nanotechnology. Biomarker Research. 2024 Nov 13;12(1):136.
3. Wu J, Chen Y, Xie M, Yu X, Su C. cGAS-STING signaling pathway in lung cancer: Regulation on antitumor immunity and application in immunotherapy. Chinese Medical Journal Pulmonary and Critical Care Medicine. 2024 Dec 30;2(04):257-64.
4. Quiros-Roldan E, Sottini A, Natali PG, Imberti L. The Impact of Immune System Aging on Infectious Diseases. Microorganisms. 2024 Apr 11;12(4):775.
5. Etienne C, Vilcu AM, Finet F, Chawki S, Blanchon T, Steichen O, Hanslik T. Incidence of serious respiratory tract infections and associated characteristics in a population exposed to immunosuppressive therapies: a register-based population study. BMC Infectious Diseases. 2024 Oct 21;24(1):1184.
6. Baker B, Hung F, Smith MJ, Erkanli A, Greenhill K, Hayes J, Parish A, Zhou G, Moorthy GS, Deri CR. Utility of Methicillin-Resistant Staphylococcus aureus Nasal PCR Testing in Pediatric Patients With Suspected Respiratory Infections. Journal of the Pediatric Infectious Diseases Society. 2024 Apr 1;13(4):242-5.
7. Nandhini P, Kumar P, Mickymaray S, Alothaim AS, Somasundaram J, Rajan M. Recent developments in methicillin-resistant Staphylococcus aureus (MRSA) treatment: A review. Antibiotics. 2022 Apr 29;11(5):606.
8. Dutta Gupta Y, Mackeyev Y, Krishnan S, Bhandary S. Mesoporous silica nanotechnology: promising advances in augmenting cancer theranostics. Cancer Nanotechnology. 2024 Dec;15(1):9.
9. Mourad DF, Radwan S, Hamdy R, Elkhashab DM, Kamel MM, Abdel-Moneim AS, Kadry DY. Identification of

Lower Respiratory Tract Pathogens in Cancer Patients: Insights into Fatal Outcomes. Microorganisms. 2024 Aug 16;12(8):1686.

10. Mustafa M, Ahmad R, Tantry IQ, Ahmad W, Siddiqui S, Alam M, Abbas K, Hassan MI, Habib S, Islam S. Apoptosis: a comprehensive overview of signaling pathways, morphological changes, and physiological significance and therapeutic implications. Cells. 2024 Nov 6;13(22):1838.
11. Castaño-Cerezo S, Pastor JM, Renilla S, Bernal V, Iborra JL, Cánovas M. An insight into the role of phosphotransacetylase (pta) and the acetate/acetyl-CoA node in Escherichia coli. Microbial cell factories. 2009 Dec;8:1-9.
12. Dash UC, Bhol NK, Swain SK, Samal RR, Nayak PK, Raina V, Panda SK, Kerry RG, Duttaroy AK, Jena AB. Oxidative stress and inflammation in the pathogenesis of neurological disorders: Mechanisms and implications. Acta Pharmaceutica Sinica B. 2024 Oct 16.
13. Pérez-Cobas AE, Ginevra C, Rusniok C, Jarraud S, Buchrieser C. The respiratory tract microbiome, the pathogen load, and clinical interventions define the severity of bacterial pneumonia. Cell Reports Medicine. 2023 Sep 19;4(9).
14. Kakoullis L, Papachristodoulou E, Chra P, Panos G. Mechanisms of antibiotic resistance in important gram-positive and gram-negative pathogens and novel antibiotic solutions. Antibiotics. 2021 Apr 10;10(4):415.
15. Hetta HF, Ramadan YN, Rashed ZI, Alharbi AA, Alsharef S, Alkindy TT, Alkhamali A, Albalawi AS, Battah B, Donadu MG. Quorum Sensing Inhibitors: An Alternative Strategy to Win the Battle against Multidrug-Resistant (MDR) Bacteria. Molecules. 2024 Jul 24;29(15):3466.
16. Zand A, Enkhbilguun S, Macharia JM, Varajti K, Szabó I, Gerencsér G, Tisza BB, Raposa BL, Gyöngyi Z, Varjas T. Betanin Attenuates Epigenetic Mechanisms and UV-Induced DNA Fragmentation in HaCaT Cells: Implications for Skin Cancer Chemoprevention. Nutrients. 2024 Mar 16;16(6):860.
17. Thiruvengadam M, Chung IM, Samynathan R, Chandar SH, Venkidasamy B, Sarkar T, Rebezov M, Gorelik O, Shariati MA, Simal-Gandara J. A comprehensive review of beetroot (Beta vulgaris L.) bioactive components in the food and pharmaceutical industries. Critical Reviews in Food Science and Nutrition. 2024 Jan 25;64(3):708-39.
18. Elfadadny A, Ragab RF, AlHarbi M, Badshah F, Ibáñez-Arancibia E, Farag A, Hendawy AO, De los Ríos-Escalante PR, Aboubakr M, Zakai SA, Nageeb WM. Antimicrobial resistance of Pseudomonas aeruginosa: navigating clinical impacts, current resistance trends, and innovations in breaking therapies. Frontiers in Microbiology. 2024 Apr 5;15:1374466.
19. Chrystle M, Vishak A, Sindhu K, Jane M. Primary lung abscess due to multidrug-resistant Klebsiella pneumoniae. BMJ Case Reports CP. 2021 Sep 1;14(9):e244759.
20. Ragavendran C, Imath M, Kamaraj C, Nakouti I, Manoharadas S. Eco-friendly synthesis of betanin-conjugated zinc oxide nanoparticles: antimicrobial efficacy and apoptotic pathway activation in oral cancer cells. Molecular Biology Reports. 2024 Dec;51(1):1128.
21. Younis FA, Saleh SR, El-Rahman SS, Newairy AS, El-Demellawy MA, Ghareeb DA. Preparation, physicochemical characterization, and bioactivity evaluation of berberine-entrapped albumin nanoparticles. Scientific Reports. 2022 Oct 19;12(1):17431.
22. Rafe Hatshan M, Perianaika Matharasi Antonyraj A, Marunganathan V, Rafi Shaik M, Deepak P, Thiyagarajulu N, Manivannan C, Jain D, Melo Coutinho HD, Guru A, Arockiaraj J. Synergistic Action of Vanillic Acid-Coated Titanium Oxide Nanoparticles: Targeting Biofilm Formation Receptors of Dental Pathogens and Modulating Apoptosis Genes for Enhanced Oral Anticancer Activity. Chemistry & Biodiversity. 2024:e202402080.
23. Nainangu P, Mothilal SN, Subramanian K, Thanigaimalai M, Kandasamy R, Srinivasan GP, Gopal S, Shaik MR, Kari ZA, Guru A, Antonyraj AP. Characterization and antibacterial evaluation of Eco-friendly silver nanoparticles synthesized by halophilic Streptomyces rochei SSCM102 isolated from mangrove sediment. Molecular Biology Reports. 2024 Dec;51(1):730.
24. Tayyeb JZ, Priya M, Guru A, Kishore Kumar MS, Giri J, Garg A, Agrawal R, Mat KB, Arockiaraj J. Multifunctional curcumin mediated zinc oxide nanoparticle enhancing biofilm inhibition and targeting apoptotic specific pathway in oral squamous carcinoma cells. Molecular Biology Reports. 2024 Dec;51(1):423.
25. Shaik MR, Ramasamy M, Jain D, Muthu K, Manivannan C, Hussain SA, Deepak P, Thiyagarajulu N, Guru A, Antonyraj AP, Coutinho HD. A Dual Approach by Nanostructured α-Mangostin-Copper Oxide Complexes Against Dental Pathogen Biofilms and Oral Cancer via Apoptosis Gene Modulation. Chemistry & Biodiversity.:e202401961.
26. Hussain SA, Ramasamy M, Shaik MR, Shaik B, Deepak P, Thiyagarajulu N, Matharasi Antonyraj AP, Guru A. Inhibition of Oral Biofilms and Enhancement of Anticancer Activity on Oral Squamous Carcinoma Cells Using Caffeine-Coated Titanium Oxide Nanoparticles.

Chemistry & Biodiversity.:e202402476.

27. Ahmad A, Tiwari RK, Almeleebia TM, et al (2021) Swertia chirayita suppresses the growth of non-small cell lung cancer A549 cells and concomitantly induces apoptosis via downregulation of JAK1/STAT3 pathway. Saudi J Biol Sci 28:6279–6288. https://doi.org/10.1016/j.sjbs.2021.06.085
28. Zand A, Enkhbilguun S, Macharia JM, Varajti K, Szabó I, Gerencsér G, Tisza BB, Raposa BL, Gyöngyi Z, Varjas T. Betanin Attenuates Epigenetic Mechanisms and UV-Induced DNA Fragmentation in HaCaT Cells: Implications for Skin Cancer Chemoprevention. Nutrients. 2024 Mar 16;16(6):860.
29. Rafieepour A, R Azari M, Khodagholi F. Cytotoxic effects of crystalline silica in the form of micro and nanoparticles on the human lung cell line A549. Toxicology and Industrial Health. 2023 Jan;39(1):23-35.
30. Ahamed M. Silica nanoparticles-induced cytotoxicity, oxidative stress, and apoptosis in cultured A431 and A549 cells. Human & experimental toxicology. 2013 Feb;32(2):186-95.
31. Karimi T, Najmoddin N, Menhaje-Bena R. Evaluation of silica nanoparticles cytotoxicity (20-40 nm) on cancerous epithelial cell (A549) and fibroblasts cells of human normal lung fibroblast (MRC5). Occupational Medicine. 2021 Apr 3.